Li Yang[1]
Minglin Li[2]
Yanli Qu[2]
Zaili Dong[2]
Wen J. Li[1]

[1]Centre for Micro and Nano Systems, The Chinese University of Hong Kong, Hong Kong
[2]State Key Laboratory of Robotics, Shenyang Institute of Automation, Chinese Academy of Sciences, Shenyang, P. R. China

Received February 28, 2009
Revised June 20, 2009
Accepted June 24, 2009

Research Article

Carbon nanotube-sensor-integrated microfluidic platform for real-time chemical concentration detection

This paper presents the development of a chemical sensor employing electronic-grade carbon nanotubes (EG-CNTs) as the active sensing element for sodium hypochlorite detection. The sensor, integrated in a PDMS-glass microfluidic chamber, was fabricated by bulk aligning of EG-CNTs between gold microelectrode pairs using dielectrophoretic technique. Upon exposure to sodium hypochlorite solution, the characteristics of the carbon nanotube chemical sensor were investigated at room temperature under constant current mode. The sensor exhibited responsivity, which fits a linear logarithmic dependence on concentration in the range of 1/32 to 8 ppm, a detection limit lower than 5 ppb, while saturating at 16 ppm. The typical response time of the sensor at room temperature is on the order of minutes and the recovery time is a few hours. In particular, the sensor showed an obvious sensitivity to the volume of detected solution. It was found that the activation power of the sensor was extremely low, *i.e.* in the range of nanowatts. These results indicate great potential of EG-CNT for advanced nanosensors with superior sensitivity, ultra-low power consumption, and less fabrication complexity.

Keywords:
Carbon nanotubes / Chemical sensor / Dielectrophoresis / Microfluidic system / Sodium hypochlorite
DOI 10.1002/elps.200900126

1 Introduction

Sodium hypochlorite (NaOCl), as a mass production chemical, is widely used for bleaching, disinfection of municipal water, sewage, food industry, chemical synthesis, pulp, and paper industry. NaOCl is a strong oxidant with causticity, and its solution is hazardous, which could burn skin or damage eyes on contact. Numerous chemical compounds such as hypochlorite ingredients routinely used in various fields of human activity can form persistent poisonous residues in air, soil, and water, thus causing lasting pollution. The leakage of NaOCl is reported occasionally in industry and jeopardizes both environment and workers' health, and it could be especially harmful if the end is human consumption or the production of foodstuffs. Therefore, it is important to introduce certain methodologies to detect the existence of hypochlorite in drinking water, foods as well as industrial wastewaters.

Volumetric and redox titration methods were used for routine analysis in laboratories to precisely determine the existence of hypochlorite traditionally [1]. These methods not only required several steps with the usage of harmful reagents but also needed spectrophotometric equipment for time-consuming analysis. Later, Soldatkin *et al.* introduced a potentiometric enzyme sensor for hypochlorite species detection, by evaluating the effect of the inhibition of the enzyme activity induced by hypochlorite species [2]. It was reported that acetylcholinesterase, a kind of enzyme, showed the best sensitivity to hypochlorite in terms of dynamic range from 0.02 to 1 mM. However, this method required a long time for the soaking process and certain immobilized enzyme, which was inconvenient as well. Furthermore, its dynamic range is also not satisfactory. Ordeig *et al.* demonstrated an electrochemical method to effectively detect hypochlorite component in fluid tap water by using bare platinum electrodes [3]. The method could provide quick and reliable analytical data with little or no sample preparation. The limit of detection was 0.07 ppm and inaccurate sensitivity was observed beyond 2.5 ppm. The drawback of this method is that platinum oxides over the electrodes surface were formed by simple contact of the platinum surface with a hypochlorite solution during the electrochemical reduction of hypochlorite ions.

Correspondence: Professor Wen J. Li, Department of Mechanical and Automation Engineering, MMW Engineering Building, The Chinese University of Hong Kong, Shatin, N. T., Hong Kong SAR, P. R. China
E-mail: wen@mae.cuhk.edu.hk
Fax: +852-2603-6002

Abbreviations: ac, alternating current; **CNTs,** carbon nanotubes; **DEP,** dielectrophoresis; **EG-CNTs,** electronic-grade carbon nanotubes; **MWNTs,** multi-walled nanotubes; **NaOCl,** sodium hypochlorite; **NH_3,** ammonia; **NO_2,** nitrogen dioxide; **SWNTs,** single-walled nanotubes

© 2009 WILEY-VCH Verlag GmbH & Co. KGaA, Weinheim

With the rapid progress and improvement of nanotechnology, sensors fabricated by using carbon nanotubes (CNTs) as the sensing element were reported to give electrical response to different chemicals, such as NO_2, NH_3, CO, H_2, and O_3 for gas detection [4–9]. CNT sensors provide high sensitivity, low power, and portable tools for *in situ* chemical analysis. So far, semiconducting sensors, normally constructed in transistor or field-effect transistor form with CNTs distributed on thin film [10–15], are the most studied application of CNTs for detecting chemical gases. When the gas molecules are absorbed on the CNTs, there will be charge transfer between the CNT sensor and the molecules; thus the conductance of the sensor is changed. Most of these sensors utilized single-walled nanotubes (SWNTs) as sensing element for detecting the molecules. The sensor responded to NO_2 *via* an increase of conductance and NH_3 *via* a decrease of conductance. The phenomenon was elaborated by Kong *et al.* in 2000 [16]. NO_2 molecules, as a kind of oxidant, withdraw electrons from CNT and leave holes on it. As a result, the electrical properties of CNT will be changed. In 2001, Chen *et al.* showed that SWNTs appear hole doped in air as a result of donating electrons to oxygen molecules. The responses to different kinds of gas molecules are different due to the difference of binding energy and charge transfer from the molecule to the CNT [17]. These CNT-based chemical sensors can operate at room temperature and give responses to some gases with both high sensitivity of several parts *per* billion [18] and fast response time of several seconds [19]. However, few CNT sensors were used to detect chemical reagents in liquid form using the microfluidic system. To achieve this, certain methodologies to deposit and align CNTs between electrodes need to be studied.

It has been demonstrated that dielectrophoresis (DEP) could provide a way to manipulate the CNTs effectively for separation, orientation, alignment, and positioning, and establish a good electrical connection between CNTs and the external measuring circuit [20–23]. Unlike the typical method using atomic force microscopy to manipulate CNTs one by one, DEP force can trap and fix bundled CNTs between electrodes in a fast and efficient manner, and make the batch fabrication of nanodevices using nanotubes as components, such as chemical sensor, feasible.

Our group has been studying the properties of electronic grade carbon nanotubes (EG-CNTs) as sensing elements integrated in microfluidic systems for fabricating shear stress sensors [24] as well as the sensors used to detect alcohol vapor [25]. EG-CNTs show not only remarkable sensibility but also excellent repeatability. This kind of CNT contains ultrapure individually suspended CNTs without any surfactant. In this study, we will present our recent progress on the NaOCl sensor based on EG-CNTs, which are formed by DEP force on glass substrate. Sensor performance under constant-current configuration will be evaluated, and different configurations will also be introduced to test the response to NaOCl under different situations.

2 Materials and methods

2.1 DEP theory

DEP refers to the force exerted on the induced dipole moment of an uncharged dielectric and/or conductive particle by a nonuniform electric field [26].

The time-averaged DEP force acting on the particles in an alternating current (ac) field was given by [27]

$$F_{\mathrm{DEP}} = \frac{\pi a^2 \ell}{12} \varepsilon_{\mathrm{m}} \mathrm{Re}\{f_{\mathrm{CM}}\} \nabla |E|^2 \tag{1}$$

where a and ℓ are the radius and length of the CNT, respectively, ε_{m} is the permittivity of the suspending medium, f_{CM} is the factor depending on the complex permittivities of both the particle and the medium, given by $f_{\mathrm{CM}} = \frac{\varepsilon_{\mathrm{p}}^*}{\varepsilon_{\mathrm{m}}^*} - 1$, ($\varepsilon_{\mathrm{p}}^* = \varepsilon_{\mathrm{p}} - i\sigma_{\mathrm{p}}/2\pi f$, $\varepsilon_{\mathrm{m}}^* = \varepsilon_{\mathrm{m}} - i\sigma_{\mathrm{m}}/2\pi f$). The subscript p and m, respectively, represent the particle and the medium. σ is the electrical conductivity and f is the frequency of the applied electric field. And finally $\nabla|E|^2$ is the gradient of square rms electric field.

Depending on the sign of $\mathrm{Re}\{f_{\mathrm{CM}}\}$, CNTs can migrate towards regions of electric field strength extrema. If the sign of $\mathrm{Re}\{f_{\mathrm{CM}}\}$ is positive, CNTs experience the positive DEP force and move towards the region with the highest electric field strength. Otherwise, CNTs experience the negative DEP force and are repelled away to the region with the lowest electric field strength.

When immersed in a dielectric solution and subjected to an electric field, CNTs are motivated to move not only by the DEP force but also by the viscous drag force due to fluid flow. For a pair of aligned finger electrodes, according to the approximate analysis in [28], the time-average electrothermal force *per* unit volume on a liquid is

$$F_E = -M\left(\frac{\varepsilon_{\mathrm{m}}\sigma_{\mathrm{m}}V^4}{8k\pi^3 r^3 T}\right)\left(1 - \frac{2\theta}{\pi}\right)\hat{n}_\theta \tag{2}$$

where M is a dimensionless factor defined by

$$M = \left(\frac{(T/\sigma_m)(\partial\sigma_m/\partial T) - (T/\varepsilon_m)(\partial\varepsilon_m/\partial T)}{1 + (2\pi f \cdot \varepsilon_m/\sigma_m)^2} + \frac{1}{2}\frac{T}{\varepsilon_m} \times \frac{\partial\varepsilon_m}{\partial T}\right) \tag{3}$$

Here, V is the potential difference across the electrodes, k the thermal conductivity of the liquid, T the absolute temperature, and r and θ are the two variables of the polar coordinate system. The origin of the polar coordinate system is located on the electrode gap center. Based on Eq. (2), the maximum of F_E appear at $\theta = 0$ and π where radial lines are parallel to the electrodes.

The dimensionless factor M accentuates the effect of electrothermal flow on the manipulation of particles using DEP technique. When M is positive, the liquid moves across the edge of electrodes from the center of electrode gap to the electrode surface. Contrarily, when M is negative, the flow direction is reversed. Moreover, the factor M varies with the frequency f of the applied electric field.

© 2009 WILEY-VCH Verlag GmbH & Co. KGaA, Weinheim

Note that particles suspended in the liquid are not directly subjected to the electrothermal force, but the drag force induced by the electrothermal force. The velocity of the liquid flow can be approximately determined by $v_\ell \approx |F_E|\ell_C^2/\eta$, where ℓ_C is the characteristic length, and η is the viscosity of liquid. Accordingly, the drag force F_{drag} exerted on a particle like CNT can be expressed as

$$F_{drag} = v_\ell \cdot f_s \approx (|F_E|\ell_C^2/\eta) \cdot (6\pi\eta\ell/\ln(2\ell/a)) \quad (4)$$

where, f_s is the friction factor equal to $6\pi\eta\ell/\ln(2\ell/a)$ for a particle like CNT.

In addition to the DEP force and the drag force, the stochastic thermal force (Brownian motion) needs to be considered when the size of particles scales down to nanometer. With ''observable'' movement of particles against the random Brownian motion, the observably deterministic threshold force is defined by [29]

$$|F_B|\sqrt{\delta_t} = \sqrt{18k_B \cdot T \cdot f_s} \quad (5)$$

where k_B is the Boltzmann constant, δ_t is the time interval of observation.

According to [23], to realize the alignment of CNTs in the gap of microelectrodes to form CNT sensors, the positive DEP force is desired to attract CNTs to the edge of microelectrodes, the negative M factor is required to move the liquid and drag the CNTs toward the edges of electrodes, and the stochastic thermal force needs to be smaller than the DEP force.

There are a few additional phenomena that could influence the motion of CNTs such as electroosmosis and nanotubes interaction. Electroosmosis only contributes dominantly with the frequency range from 10 Hz to 100 kHz [29], which means that the results will be hardly affected by this factor with a much larger frequency. Although nanotubes interaction is usually not taken into account during calculation or simulation, it responsible for the formation of chains and networks of particles using DEP and bridge gaps much larger than the length of a single nanotube [29].

For a DI water consisting of dispersed CNTs, the parameters of the solution are $\sigma_p = 2.2 \times 10^4\,S/m$, $\varepsilon_m = 100\varepsilon_0$, $\varepsilon_0 = 8.85 \times 10^{-12}\,F/m$, $\ell = 10\,\mu m$, and $a = 10\,nm$ for CNTs, and $\sigma_m = 5.5 \times 10^{-6}\,S/m$, $\varepsilon_m = 80\varepsilon_0$, $k = 0.6\,W/(m^2K)$, $\eta = 0.001\,Pa \cdot s$, $(1/\sigma_m)(\partial\sigma/\partial T) = 2\%$ *per* degree, and $(1/\varepsilon_m)(\partial\varepsilon/\partial T) = -0.4$ *per* degree for DI water. With the use of a microelectrode pair of 4 μm width and 0.4 μm height and separate by 5 μm, the electric field strength E and the unit vector of $\nabla|E|^2$ can be calculated using the finite element method. Figure 1 shows the distributions of E and the unit vector of $\nabla|E|^2$ in the vertical symmetric plane of the electrode pairs. The strongest electric fields, towards which the positive DEP force will attract the CNTs to move, are located at the edges of electrodes.

Neglecting end effects, an analytical expression of E can be given by $E = V/(\pi r)\hat{n}_\theta$. Assuming $r = 2.5\,\mu m$, the forces of DEP, electrothermal flow drag and the Brownian motion can be calculated. As shown in Fig. 2, the larger voltage results in the larger DEP force and electrothermal drag force.

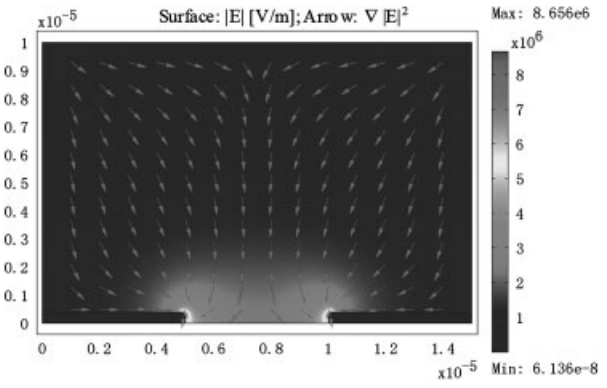

Figure 1. The field intensity distribution $|E|$ and its gradient $\nabla|E|^2$ in the symmetric vertical plane at 16 V_{p-p} and 1 MHz.

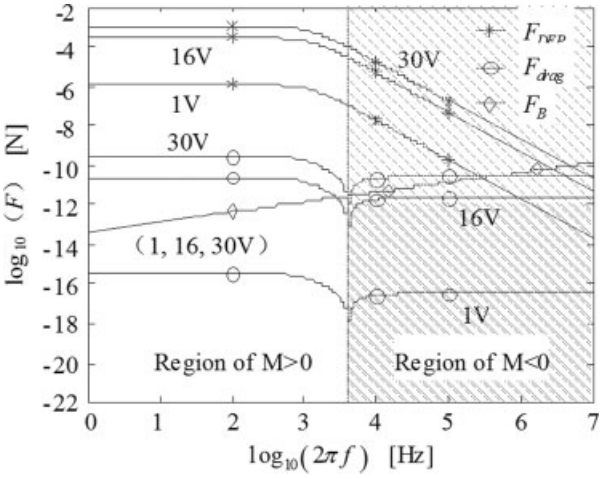

Figure 2. The forces of DEP and flow drag and Brownian motion varying along with the frequency f and the voltage V.

With an ac bias with the frequency of 1 MHz and voltage of 16 V_{p-p}, the mean value of $|\nabla|E|^2|$ in the line of electrode surface is obtained to be $1.029 \times 10^{19} V^2/m^3$. Then, the DEP force exerted on the CNT is estimated to be 1.167×10^{-8} N with the $\mathrm{Re}\{f_{CM}\} = 6.115 \times 10^3$, which indicates a positive DEP effect. For DI water, the dimensionless factor M equates to −0.6, which indicates a desired liquid movement across the edges of electrode gap from the electrode surface to the center of gap. Furthermore, the drag force that acts on CNTs transformed from the electrothermal force can be obtained to be 2.177×10^{-12} N, which is smaller than the DEP force. In addition, during a period of $\delta_t = 1/f$, the observable threshold force can also be estimated to be 4.3×10^{-11} N, still smaller than the DEP force.

2.2 Sensor fabrication

As shown in Fig. 3, the pattern of microelectrodes was etched by the wet chemical etching process after the sputtering deposition of metals on the glass substrate using

© 2009 WILEY-VCH Verlag GmbH & Co. KGaA, Weinheim

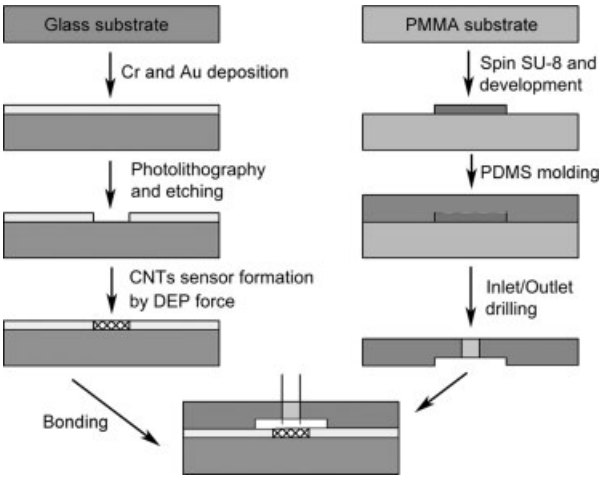

Figure 3. Fabrication process of the EG-CNTs sensor.

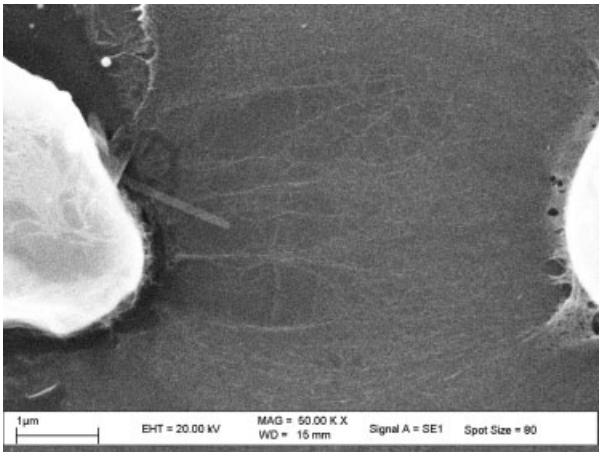

Figure 4. The SEM image of the EG-CNTs between two microelectrodes after fabrication by DEP force.

standard photolithography process. The electrodes were composed two layers: a gold layer with the thickness of ~3000 Å and an adhesion layer of chromium with the thickness of ~1000 Å between the gold layer and glass substrate. Then EG-CNTs were batch aligned between the microelectrode pair of 4 μm width and 5 μm gap distance by using DEP with an ac voltage of 16 V_{p-p} and 1 MHz. The SEM picture of the actual network is shown in Fig. 4. Finally a PDMS (SYLGARD 184 Silicone Elastomer Kit, Dow Corning, USA) channel shaped by a mold was bonded onto the glass surface to form the microchamber in which the detected solution will be confined. The length of the microchannel was 21 mm and the size of the cross section area was 1 mm × 40 μm.

2.3 Experimental setup

The experimental setup was integrated as shown in Fig. 5. A Versapump 6 (Kleoehn, USA) syringe pump, with a

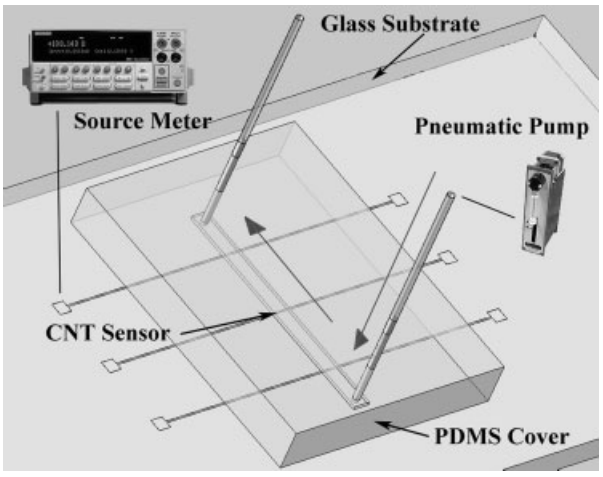

Figure 5. The experimental setup when testing the response of the CNT sensor to the injected solution.

resolution down to $\sim 5.2 \times 10^{-2}$μL *per* step, was used to precisely control the flow rate and inject the solution into the CNT sensor chip. A sourcemeter (Keithley2400, Keithley, USA) was used to generate the operating current to activate the sensor and also to provide the CNT electrical conductance values to the computer *via* its digital output port. Conductance measurements were conducted under constant current mode. During experiment, the environment was controlled at 24°C with 50% humidity. The EG-CNT sensor was first activated; meanwhile, the conductance started to be recorded. Then, the detected NaOCl solution was injected at certain flow rate and volume into the microchamber. Each measurement lasted ~20 min to permit CNT conductance to reach a steady state. Afterwards, the sensor was treated by UV illumination until the conductance recovered to the initial level before the next test.

3 Results

3.1 I–V characteristics

After annealing at 60–80°C for several hours before usage, the resistance of the sensing elements normally ranges from several hundred ohms to tens of thousand ohms at room temperature. It was reported that the nominal resistance of the sensing elements can be adjusted by annealing the multi-walled nanotubes (MWNTs) through electrical current heating, which ''burns'' off the wall(s) of MWNTs and causes an increase in nominal resistance of the sensing element [30]. The repeatable phenomenon is used to stabilize the resistance value across the sensing electrodes. In addition, the resistance may be different for different sensing elements due to the concentration and volume difference of the droplet of EG-CNTs solution.

The I–V curve of a typical EG-CNT sensor began to exhibit an obvious nonlinearity at 50 μA, as shown in Fig. 6. The deviation from the linear Ohm's law expectation,

© 2009 WILEY-VCH Verlag GmbH & Co. KGaA, Weinheim

caused possibly by self-heating effect of CNTs, became larger while input current increased. To avoid this thermal effect spoiling the measurement accuracy, the operating current was limited to lower than 10 μA, which means the power supply was not higher than 500 nW.

3.2 Typical response to NaOCl

Figure 7 shows the typical response of the EG-CNT sensor to 2 ppm NaOCl solution by three different sensing elements in the same microchannel, with identical flow rate of 1.04 m/s and volume of 55 μL. The injection process was within few seconds; hence, all the responses were measured in static solution. Since the initial conductance of each sensor is distinct (sensor A with 38 μS; sensor B with 20.8 μS; sensor C with 0.14 mS), constant current was adjusted for each sensor to let initial power consumption during the experiment to be ~100 nW. Before the introduction of solution, the CNT conductance showed a random

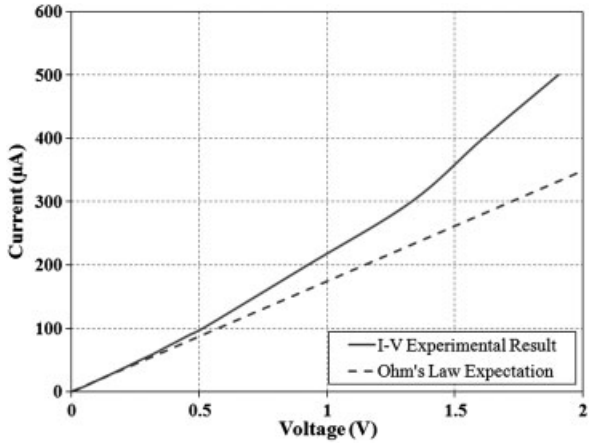

Figure 6. I–V characteristics of a typical EG-CNT sensor.

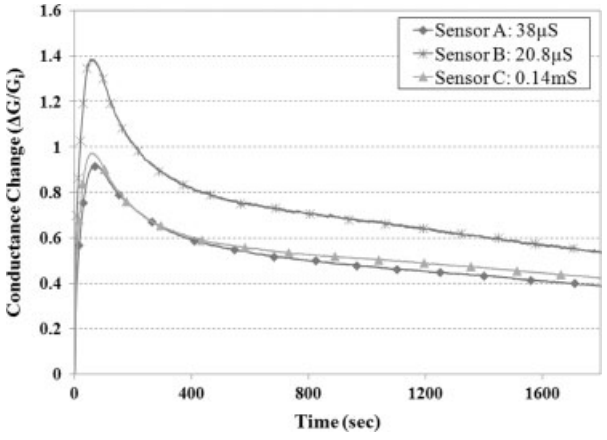

Figure 7. The typical response of three EG-CNT sensors to 2 ppm NaOCl solution from the injection; the measurement was carried out in static solution.

fluctuation with less than 0.1% resistance change. Once the solution passed over CNTs, the conductance increased sharply and reached the peak within the initial tens of seconds, while it decreased a little and stayed constant further away. All the sensors responded similarly, with difference only on the response amplitude. These tests were carried out for examining how reproducible the NaOCl detection is using different sensors.

When bare electrodes were used to carry out the experiment, *i.e.* by not having CNTs between the electrodes, only noise was recorded from the source meter due to the open circuit. The conductance values of the electrodes in DI water and NaOCl were only several nanowatts, which was too small compared with the conductance of EG-CNTs, which indicated that the signal was indeed generated by CNT conductance change.

A possible explanation for this phenomenon can be provided by studying the response of SWNT to gas molecules such as NH_3 and NO_2. When charge transfer takes place between the CNT sensor and particular molecules, there will be holes or carriers left on the CNTs. As a result, the conductance of the sensor is increased or decreased. Typical electrochemical interaction may be denoted as:

$$\begin{aligned} &\mathrm{CNT} + \mathrm{Molecule} \rightarrow \mathrm{CNT}^{\delta e}\,\mathrm{Molecule}^{\delta+} \\ &\text{or } \mathrm{CNT}^{\delta+}\mathrm{Molecule}^{\delta e} \end{aligned} \tag{6}$$

where δ is a number that indicates the amount of charge transferred during the interaction [31]; "*e*" represents electron while "+" represents holes. As NaOCl is a kind of oxidant, it is expected to respond similarly or has a trend similar to other oxidants or molecules that withdraw electrons from the CNT sensors with an increase in conductance.

3.3 Sensitivity

An EG-CNTs sensor with initial conductance of 2.9 μS was used for the concentration response tests ranging from 5 ppb to 32 ppm with flow rate of 1.04 m/s and volume of 18 μL, respectively. Therefore, the variation of each response was theoretically purely influenced by the amount of NaOCl molecules, or OCl^-, in the solution.

The sensor response patterns of NaOCl solution with concentration from 1/32 to 8 ppm were shown in Fig. 8, which proved the repeatability of the sensor when responding to this chemical. The response to solution concentration ascended consistently as the concentration increased from 1/32 ppm. The shapes of response curves were similar to the typical response described in Section 3.2, with differences only in amplitude and duration of overshoot period. As the concentration increased, the overshoot became much more obvious and with higher peak amplitude. Also, the time constant required to reach the peak was prolonged.

Figure 9 shows the response difference as a function of concentration. When the concentration was below

© 2009 WILEY-VCH Verlag GmbH & Co. KGaA, Weinheim

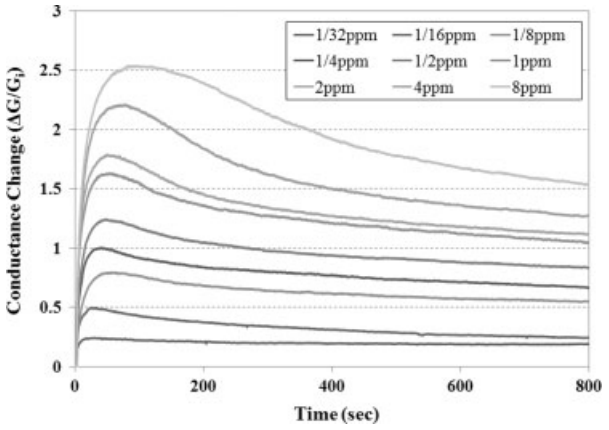

Figure 8. The sensitivity test of an EG-CNT sensor to NaOCl solution from 1/32 to 8 ppm *versus* time.

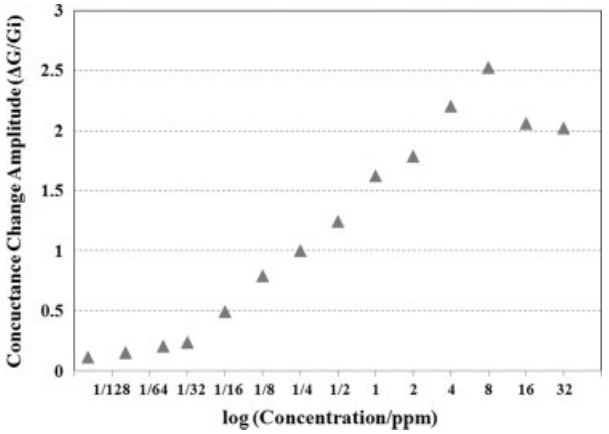

Figure 9. The maximum amplitudes of sensor response to NaOCl solution of different concentration from 5 ppb to 32 ppm.

1/32 ppm, the conductance was not as distinguishable as higher concentration response tests. For the concentration higher than 8 ppm, the responses were assumed to have saturated and the amplitudes did not show an obvious trend. The sensitivity shows best performance between 1/32 and 8 ppm, which exactly obeys the typical response and the response fits a linear logarithmic dependence on the concentration.

The ascending period for each response from 1/32 to 8 ppm can be fitted by a first-order exponential function:

$$y = Ae^{-\frac{t}{\tau}} + y_0 \quad (7)$$

Figures 10A–C show the fitted values of A, time constant τ, and y_0, respectively, as a function of concentration from 1/32 to 8 ppm. The relationship between each variable and the logarithmic concentration is linear, which indicates that the response of the EG-CNT sensor to NaOCl solution is predictable by analyzing the ascending period of the response curve. As a result, currently our sensor is capable of testing solutions with concentrations ranging from 1/32 to 8 ppm.

3.4 Effect of flow rate and volume on sensor performance

Experiments were conducted at different flow rates by using the NaOCl solution with concentrations of 1/8, 1, and 8 ppm. During the measurement, the total volume injected into the channel was fixed at 26.5 μL.

As shown in Fig. 11, the flow rate is not a major factor that affects the response of the EG-SNT sensor to NaOCl solution within the range 0.065–1.04 m/s. To test the response to different volumes, the same EG-CNT sensor was used at a flow rate of 1.56 m/s.

Here, the volume is defined as the ''total volume of the solution that has been injected to the microchannel''. The larger the value is, the more the solution is reacted with the EG-CNTs sensor, and hence the more the electron transfer should have occurred theoretically.

Figure 12 shows three groups of responses to NaOCl solution with a concentration of 0.125, 1, and 8 ppm. Five response tests were carried out for each concentration group by different volume configurations, *i.e.* 2, 6, 18, 54, and 162 μL.

For smaller concentration values such as 0.125 and 1 ppm, the response to the solution ascended as the volume

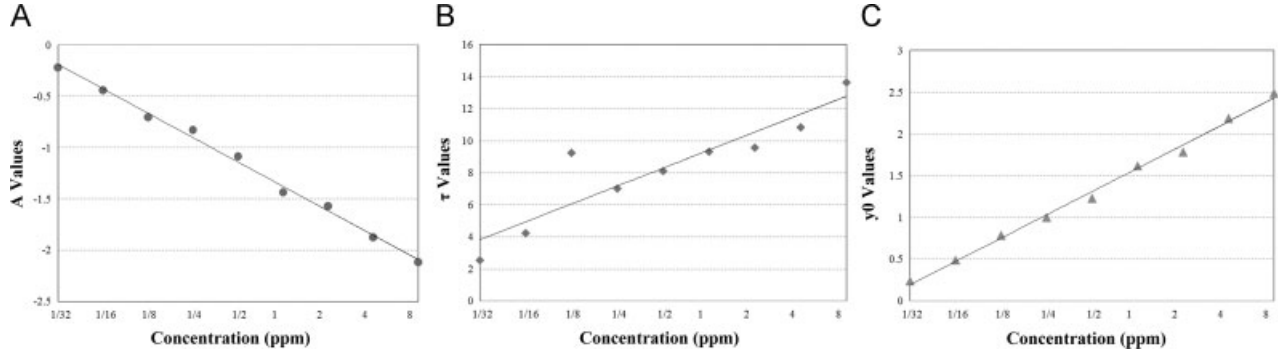

Figure 10. A–C: The fitted values of A, time constant τ and y_0 *versus* concentration, respectively.

© 2009 WILEY-VCH Verlag GmbH & Co. KGaA, Weinheim

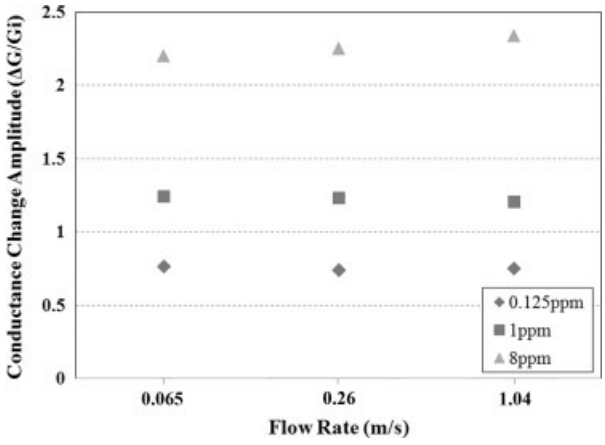

Figure 11. The flow rate test by the responses to the solution with identical volume value but different concentrations of three groups.

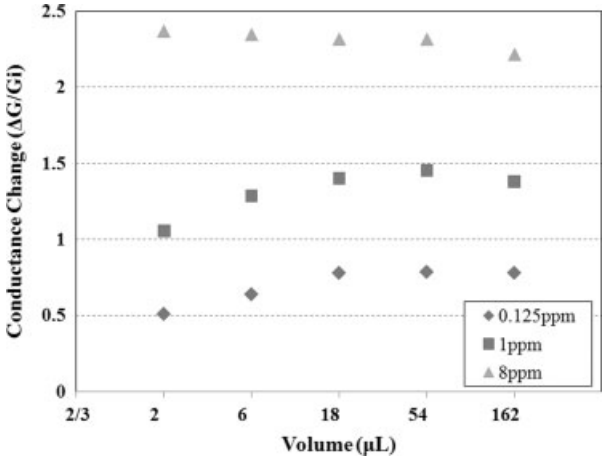

Figure 12. The volume test demonstrated by three concentration groups of 1/8, 1 and 8 ppm, with the same flow rate of 1.56 m/s.

value increased until the volume value reached 18 μL. The differences among 18, 54, and 162 μL were negligible. When the concentration of the solution was increased to 8 ppm, all five responses showed similar amplitudes of conductance change and tended to be saturated. Although the reason behind this phenomenon remains unknown, the total volume injected into the channel was set to 18 μL for all other experiments of chemical detection described henceforth. This is because, for this configuration, the amplitude of the response is expected to reach its maximum value for different concentration values.

4 Discussion

We have developed an ultra-low-powered EG-CNT sensor for NaOCl detection at room temperature by combining micro-elecro-mechanical systems compatible fabrication technology with ac DEP technique. It was found that the sensitivity of our EG-CNT sensors was lower than 5 ppb, and the output conductance of the sensor fitted a linear logarithmic concentration dependence in the range from ppb to tens of ppm. Moreover, the larger the volume passing over the EG-CNTs, the higher the response that implied the electron absorption mechanism of this chemical sensor. However, the flow rate produced little influence on the sensor response compared with chemical absorption.

We have demonstrated that the EG-CNT sensor would respond consistently to static NaOCl solution using microfluidic system and provided a methodology for reagent sensing. The sensor reacted with different response curves under different flow conditions. Although systematic explanations are difficult to list based on current results, some test configurations that may lead to errors have been found, which should be avoided in future experiments.

The authors acknowledge the support from the Hong Kong Research Grants Council (Project No.: 2050440) and the Chinese National High Tech Plan (863 Project No.: 60675060). They also acknowledge the Chemistry Department, CUHK for providing sodium hydroxide (NaOH), sodium chloride (NaCl).

The authors have declared no conflict of interest.

5 References

[1] Meites, L., *Handbook of Analytical Chemistry*, McGraw-Hill, New York 1963.

[2] Soldatkin, A. P., Gorchkov, D. V., Martelet, C., Jaffrezic-Renault, N., *Sens. Actuators B* 1997, *43*, 99–104.

[3] Ordeig, O., Mas, R., Gonzalo, J., Del Campo, F. J., Munoz, F. J., Haro, C., *Electroanalysis* 2005, *17*, 1641–1648.

[4] Lee, S. M., Lee, Y. H., *Appl. Phys. Lett.* 2000, *79*, 2877–2879.

[5] Valentini, L., Armentano, I., Kenny, J. M., Cantalini, C., Lozzi, L., Santucci, S., *Appl. Phys. Lett.* 2003, *82*, 961–963.

[6] Li, J., Lu, Y., Ye, Q., Cinke, M., Han, J., Meyyappan, M., *Nano Lett.* 2003, *3*, 929–933.

[7] Varghese, O. K., Kichambre, P. D., Gong, D., Ong, K. G., Dickey, E. C., Grimes, C. A., *Sens. Actuators B* 2001, *81*, 32–41.

[8] Chopra, S., Pham, A., Gaillard, J., Parker, A., Rao, A. M., *Appl. Phys. Lett.* 2002, *80*, 4632–4634.

[9] Picozzi, S., Lozzi, L., Santucci, S., Cantalini, C., Baratto, C., Sberveglieri, G., Armentano, I. *et al.*, *J. Vacuum Sci. Tech.* 2004, *22*, 1466–1470.

[10] Kazaoui, S., Minami, N., Yamawaki, H., Aoki, K., Kataura, H., Achiba, Y., *Phys. Rev. B* 2000, *62*, 1643–1646.

[11] Valentini, L., Cantalini, C., Armentano, I., Kenny, J. M., Lozzi, L., Santucci, S., *Diam. Rel. Mater.* 2004, *13*, 1301–1305.

© 2009 WILEY-VCH Verlag GmbH & Co. KGaA, Weinheim

[12] Unalan, H. E., Fanchini, G., Kanwal, A., Pasquier, A. D., Chhowalla, M., *Nano Lett.* 2006, *6*, 677–682.

[13] Penza, M., Tagliente, M. A., Aversa, P., Re, M., Cassano, G., *Nanotechnology* 2007, *18*, 185502, 1–12.

[14] Someya, T., Small, J., Kim, P., Nuckolls, C., Yardley, J. T., *Nano Lett.* 2003, *3*, 877–881.

[15] Na, P. S., Kim, H., So, H. M., Kong, K. J., Chang, H., Ryu, B. H., Choi, Y. *et al.*, *Appl. Phys. Lett.* 2005, *87*, 093101–093103.

[16] Kong, J., Franklin, N. R., Zhou, C., Chapline, M. G., Peng, S., Cho, K., Dai, H., *Science* 2000, *287*, 622–625.

[17] Chen, R. J., Franklin, N. R., Kong, J., Cao, J., Tombler, T. W., Zhang, Y., Dai, H., *Appl. Phys. Lett.* 2001, *79*, 2258–2260.

[18] Qi, P., Vermesh, O., Grecu, M., Javey, A., Wang, Q., Dai, H., Peng, S., Cho, K. J., *Nano Lett.* 2003, *3*, 347–351.

[19] Tran, T. H., Lee, J. W., Lee, K., Lee, Y. D., Ju, B. K., *Sens. Actuators B* 2008, *129*, 67–71.

[20] Chen, X. Q., Saito, T., Yamada, H., Matsushige, K., *Appl. Phys. Lett.* 2001, *78*, 3714–3716.

[21] Wakaya, F., Nagai, T., Gamo, K., *Microelec. Eng.* 2002, *63*, 27–31.

[22] Chan, H. M., Fung, K. M., Li, W. J., *Nanotechnology* 2004, *15*, S672–S677.

[23] Tung, S., Rokadia, H., Li, W. J., *Sens. Actuators A* 2007, *133*, 431–438.

[24] Qu, Y., Chow, W. Y., Ouyang, M., Tung, S., Li, W. J., Han, X., *IEEE Trans. Nanotechnol.* 2008, 565–572.

[25] Sin, L. Y., Chow, C. T., Wong, M. K., Li, W. J., Leong, H. W., Wong, K. W., *IEEE Trans. Nanotechnol.* 2007, 571–577.

[26] Pohl, H. A., Ackland, H., *Dielectrophoresis: The Behavior of Neutral Matter in Nonuniform Electric Fields*. Cambridge University Press, Cambridge 1987.

[27] Dimaki, M., Boggild, P., *Nanotechnology* 2004, *15*, 1095–1102.

[28] Ramos, A., Morgan, H., Green, N. G., Castellanos, A., *J. Phys. D Appl. Phys.* 1998, *31*, 2338–2353.

[29] Morgan, H., Green, N. G., *AC Electrokinetics: Colloids and Nanoparticles*, Research Studies Press Ltd, Philadelphia 2003, p. 170.

[30] Fung, K. M., Zhang, Q. H., Chan, H. M., Li, W. J., *18th IEEE International Conference on MEMS* 2005, 251–254.

[31] Meyyappan, M., *Carbon Nanotubes: Science and Applications*, CRC Press, Boca Raton 2004, pp. 213–236.

© 2009 WILEY-VCH Verlag GmbH & Co. KGaA, Weinheim